

# Improved real-time bio-aerosol classification using Artificial Neural Networks

Maciej Leśkiewicz<sup>1</sup>, \*Miron Kaliszewski<sup>2</sup>, Maksymilian Włodarski<sup>2</sup>, Jarosław Młyńczak<sup>2</sup>, Zygmunt Mierczyk<sup>2</sup>, Krzysztof Kopczyński<sup>2</sup>.

1. PCO S.A. ul. Jana Nowaka-Jeziorańskiego 28, 03-982 Warsaw, Poland.
2. Institute of Optoelectronics, Military University of Technology, ul. Gen. Witolda Urbanowicza 2, 00-908 Warsaw, Poland

\*Corresponding author: miron.kaliszewski@wat.edu.pl

**Keywords: Bio-aerosol, Fluorescence, Real-time analysis, Artificial Neural Network, PBAP.**

## 1. Abstract

Air pollution has had an increasingly powerful impact on the everyday life of humans. Ever more people are aware of the health problems that may result from inhaling air which contains dust, bacteria, pollens or fungi. There is a need for real-time information about ambient particulate matter. Devices currently available on the market can detect some particles in the air but cannot classify them according to health threats. Fortunately, a new type of technology is emerging as a promising solution.

Laser based bio-detectors are opening a new era in aerosol research. They are capable of characterizing a great number of individual particles in seconds by analyzing optical scattering and fluorescence characteristics. In this study we demonstrate the application of Artificial Neural Networks (ANNs) to real-time analysis of single particle fluorescence fingerprints acquired using BARDet (a Bio-AeRosol Detector). 48 different aerosols including pollens, bacteria, fungi, spores, and non-biological substances were characterized. An entirely new approach to data analysis using a decision tree comprising 22 independent neural networks was discussed. Applying confusion matrices and ROC analysis the best sets of ANNs for each group of similar aerosols was determined. As a result, a very high accuracy of aerosol classification in real-time was achieved. It was found that for some substances that have characteristic spectra almost each particle can be properly classified. Aerosols with similar spectral characteristics can be classified specific clouds with high probability. In both cases the system recognized aerosol type with no mistakes.

In the future, it is planned that performance of the system may be determined under real environmental conditions, involving characterization of fluorescent and non-fluorescent particles.

## 2. Introduction

Ambient air contains a variety of particles such as dust, bacteria, pollens, fungi and other particles of biological and non-biological origin (Pöhlker et al., 2013; Górny, 2004). Aerosols are involved in various atmospheric processes such as ice nuclei formation, precipitation and global climate effects (Deguillaume et al., 2008; Fröhlich-Nowoisky et al., 2016; Gabey et al., 2010; Pósfai and Buseck, 2010; Fuzzi et al., 2015). They also greatly influence human health (Davidson et al., 2005; Pope and Dockery, 2006; Michaels, 2017; Shiraiwa et al., 2012). Therefore, the characterization of ambient air is important for estimating potential health hazards and environmental impact (Mauderly and Chow, 2008; Lim et al., 2005). Standard methods of aerosol composition assessment usually include microscopic inspection or molecular analysis of filters (Miaskiewicz-Peska and Lebkowska, 2012), tape or liquid trapped particles. Nevertheless, they suffer from low time

47 resolution due to periodical and relatively long analytical procedures. They are also ineffective for the  
48 detection of non-culturable microorganisms (Blais-Lecours et al., 2015; Trafny et al., 2014).

49 The detection and classification of biological particles is possible using fluorescence techniques  
50 due to the presence of proteins, NADH, and some vitamins that emit light when excited with UV light  
51 (Lakowicz, 2006). This feature is utilized in single particle fluorescence detectors. In the flowing air  
52 each particle is characterized for size/shape using light scattering as well as fluorescence properties.  
53 This approach ensures continuous measurement and immediate response. Thus the analysis process  
54 can be facilitated and accelerated compared with other commonly used analytical procedures (Hill et  
55 al., 1999; Choi et al., 2014; Taketani et al., 2013; Feugnet et al., 2008). Besides advantages such as  
56 reagentless and real time particle characterization, the laser based methods do not provide  
57 information on the chemical composition of aerosol.

58 Several studies using single particle fluorescence detectors have demonstrated that fluctuations  
59 of aerosol concentration and variations in its fluorescence properties are highly dependent on the  
60 season, day, time, location and place occupancy (Gabey et al., 2011; Huffman et al., 2010; Pinnick et  
61 al., 2004; Bhangar et al., 2014; Fennelly et al., 2017). Each single particle passing the instrument is  
62 labelled with a time stamp, scattering properties (size and/or shape) and fluorescence  
63 characteristics. It is obvious that continuous single particle measurements bring a new potential and  
64 quality to environmental research. However, particles of the same type and batch display slightly  
65 different spectral characteristics due to variations in biochemical composition, size, age of population  
66 (Agranovski et al., 2003), degradation (Hernandez et al., 2016) or stress level (Lee et al., 2010) and  
67 the particle position within the instrument's interrogation point (Pan et al., 2011). Simpler statistical  
68 analyses, such as data averaging and graphical spectra representation, are not sufficient. Therefore,  
69 the huge amount of data and occurring spectral variations require more advanced algorithms  
70 supporting automatic data classification. Various analytical methods of particle discrimination and  
71 classification have been applied. It has been shown that Principal Component Analysis (PCA), Linear  
72 Discriminant Analysis (LDA), Hierarchical cluster Analysis (HCA) of fluorescence spectra greatly  
73 increase discrimination of particles compared with methods based on spectra averaging or  
74 fluorescence threshold (Leśkiewicz et al., 2016; Kaliszewski et al., 2013; Pan et al., 2012; Savage et al.,  
75 2017; Crawford et al., 2015). Artificial neural networks (ANNs) comprise an emerging analytical  
76 approach that is becoming more widely and successfully applied in various life domains such as  
77 chemical analysis (Borecki et al., 2008), image recognition (Antowiak and Chałasińska-Macukow,  
78 2003), data mining and weather forecasting (Purnomo et al., 2017). It has been shown that ANNs can  
79 be applied in bio-aerosol classification (Kohlus and Bottlinger, 1993). However, it usually requires  
80 more user input compared to other analytical procedures (Ruske et al., 2017).

81 This paper focuses on the application of ANNs for real time discrimination of bio-aerosols based  
82 on single particle fluorescence characteristics. We demonstrate a new approach to data analysis  
83 using ANNs which allows automation of data preparation procedures and minimum user  
84 involvement.

85

### 86 **3. Materials and methods**

#### 87 **3.1. Experiment**

##### 88 **3.1.1. BioAeRosol Detector (BARDet)**

89 Detailed information concerning the construction and parameters of the instrument used for  
90 the experiments was presented in our previous work (Kaliszewski et al., 2016). In general, the  
91 ambient air is continuously drawn through the nozzle. It is focused with a sheath flow of filtered air.

92 Particles in the focused air pass through the BARDet’s chamber where they are interrogated by a  
 93 16mW CW laser beam generated by a diode laser operating at 375 nm wavelength (CUBE, Coherent).  
 94 The backward and forward scattered signals are detected with two PMTs (H6780, Hamamatsu)  
 95 mounted at the 35° and 145° angles to the laser beam axis.

96 The fluorescence of particles is measured at a 90° angle to the laser beam with 32 channel PMT  
 97 (A10766, Hamamatsu). The longpass filter with cutting edge at 400 nm (Edmund Optics) separates  
 98 the fluorescence signal from scattered light. The multichannel PMT measures fluorescence in 18  
 99 active channels in a range of 415.4-643.5 nm. The channels are grouped in 7 bands. Such a solution  
 100 extends the dynamic range of measured spectra and, assures a high S/N ratio, and also reduces the  
 101 possibility of signal saturation. The remaining channels are not used. The band configuration is  
 102 presented in Table 1.

103  
 104 Table 1. Configuration of bands in the multichannel PMT.  
 105

BARDet’s Fluorescence Bands	Bandwidth [nm]
B1	415.4 – 429.3
B2	443.1 – 456.8
B3	470.5 – 484.2
B4	497.8 – 524.9
B5	538.3 – 565.0
B6	578.3 – 604.6
B7	617.6 – 643.5

106  
 107 **3.1.2. Aerosols**

108 For the tests, dry powders of harmless substances were used since they did not need a  
 109 specialized aerosol protection chamber. In order to achieve a reliable aerosol classification, the ANNs  
 110 need to be trained possibly using a large number of measurement data. Therefore, various particle  
 111 types, that can be easily aerosolized, were tested. Samples such as pollens, fungi, bacteria, spores  
 112 and plant debris naturally occur in the atmosphere. Biofluorophores such as riboflavin, cellulose,  
 113 amino acids and proteins were also characterized since they are present in biological materials. The  
 114 group of bacterial growth media was investigated due to their powerful influence on bacteria  
 115 fluorescence especially if they are not sufficiently washed. This can occur in the case of intentionally  
 116 released bacterial aerosols. Due to technical limitations, samples other than pharmaceutical could  
 117 not be aerosolized in this study. The aerosols of flours, and fluorescent non-biological substances  
 118 such as paper dust, AC fine Test Dust and talc were analyzed since they can occur especially in indoor  
 119 and public places. Non-fluorescent particles were not a subject of the research since they can be  
 120 automatically discarded as non-biologically applying given fluorescence thresholds.

121 The samples used for this study are listed in Table 2. To perform numerous experiments,  
 122 disposable vials were used, one for each aerosol sample. This prevented cross contamination  
 123 between measured samples. The aerosols were generated from modified 50 ml Falcon tubes placed

124 on the vortex. The vials in the lower part contained two connectors for silicon tubes. Vortexed  
 125 particles were entrained and formed an aerosol cloud inside the Falcon tube. The aerosolized  
 126 particles were aspirated from the vial to BARDet's aerosol inlet. Each tube contained about 50 mg of  
 127 the dry powder sample. During aerosol generation, filtered air was supplied into the vial to  
 128 compensate for the BARDet's flow. The concentration of the aerosols was adjusted with vibration  
 129 frequency of the vortex. The measurement started after the aerosol reached a homogeneous  
 130 concentration. The experimental setup is shown in Figure 1.

131

132 Table 2. List of all substances used in the experiment.

133

	Abbreviation	Name	Size [ $\mu\text{m}$ ]	AF	Source	Group
1	FM	Fluoromax green fluorescent 7 $\mu\text{m}$ microspheres	6.25 $\pm$ 0.91	0.92 $\pm$ 0.02	Thermo scientific	standard 1
2	RIB	Riboflavin	2.22 $\pm$ 1.82	0.88 $\pm$ 0.09	Sigma-Aldrich	standard 2
3	BGP	<i>Cynodon dactylon</i> (Bermuda grass)	28.35 $\pm$ 0.6	0.97 $\pm$ 0.01	Duke Sci. Corp.	pollens
4	CP	Zea mays (Corn)	78.13 $\pm$ 1.22	0.95 $\pm$ 0.01	Duke Sci. Corp.	
5	CA	<i>Corylus avellana</i> (Common hazel)	27.71 $\pm$ 1.33	0.67 $\pm$ 0.04	(*OC)	
6	LP	<i>Lycopodium</i>	30.67 $\pm$ 1.2	0.94 $\pm$ 0.01	Fluka	
7	PPP	<i>Poa pratensis</i> (Kentucky bluegrass)	30.62 $\pm$ 0.87	0.94 $\pm$ 0.01	Sigma-Aldrich	
8	RP	<i>Ambrosia</i> (Ragweed)	19.48 $\pm$ 0.78	0.99 $\pm$ 0.01	Duke Sci. Corp.	
9	SCP	<i>Secale cereale</i> (Rye)	44.8 $\pm$ 2.01	0.94 $\pm$ 0.01	Sigma-Aldrich	
10	SP	<i>Picea</i> (Spruce)	70.09 $\pm$ 4.16	0.88 $\pm$ 0.02	(*OC)	
11	AA	<i>Abies alba</i> (Silver fir)	84.56 $\pm$ 12.77	0.92 $\pm$ 0.02	(*OC)	
12	UDP	<i>Urtica dioica</i> (Common nettle)	14.99 $\pm$ 1.26	0.9 $\pm$ 0.05	(*OC)	
13	PSP	<i>Pinus sylvestris</i> (Scots pine)	39.29 $\pm$ 1.44	0.93 $\pm$ 0.02	(*OC)	
14	PNP	<i>Pinus nigra</i> (Black pine)	44.97 $\pm$ 1.33	0.88 $\pm$ 0.03	(*OC)	
15	LPP	<i>Lycopodium</i> (Poland)	28.66 $\pm$ 0.6	0.95 $\pm$ 0.01	(*OC)	
16	PMP	<i>Broussonetia papyrifera</i> (Paper mulberry)	13.57 $\pm$ 0.88	0.94 $\pm$ 0.04	Duke Sci. Corp.	
17	ATP	<i>Artemisia tridentata</i> (Big Sagebrush)	22.53 $\pm$ 0.42	0.96 $\pm$ 0.01	Sigma-Aldrich	
18	AAP	<i>Artemisia absinthium</i> (Wormwood)	18.37 $\pm$ 1.51	0.96 $\pm$ 0.02	Sigma-Aldrich	
19	CPP	<i>Chenopodium</i>	27.29 $\pm$ 0.97	0.98 $\pm$ 0.01	(*OC)	
20	BWF	Buck wheat flour	25.17 $\pm$ 15.76	0.82 $\pm$ 0.06	MELVIT Poland (*RS)	flours
21	PF	Potato flour	21.23 $\pm$ 3.11	0.96 $\pm$ 0.03	KUPIEC Poland (*RS)	

22	RF	Rice flour	18.22±6.23	0.6±0.07	MELVIT Poland (*RS)	
23	TF	Tapioca flour	12.91±3.41	0.7±0.06	COCK BRAND (*RS)	
24	WF	Wheat flour	20.57±4.36	0.62±0.07	MELVIT Poland (*RS)	
25	Trp	Tryptophan	15.42±8.96	0.81±0.08	Sigma-Aldrich	amino acids and proteins
26	Phe	Phenylalanine	10.41±5.31	0.73±0.11	Sigma-Aldrich	
27	BSA	Bovine Serum Albumin	63.8±30.49	0.43±0.05	POCH Poland	
28	OVA	Ovalbumin	26.45±5.31	0.83±0.07	POCH Poland	
29	AMBAMB	<i>Bif. animalis</i> , <i>S. boulardii</i> , <i>S. thermophilus</i> , <i>L. casei</i> , <i>L. bulgaricus</i>	27.97±4.42	0.84±0.03	AMBIO Probiotyky, Lab. Galenowe Poland (*P)	bacteria in medium
30	LCB	<i>Lactobacillus bulgaricus</i>	51.16±19.33	0.68±0.08	LakciBios, ASA Poland (*P)	
31	LF	<i>Bifidobacterium animalis</i> , <i>L. acidophilus</i>	32.62±8.45	0.82±0.07	Linex forte, LEK Pharmaceuticals d.d. Slovenia (*P)	
32	BA	Bacteriological Agar	49.47±10.03	0.74±0.07	Sigma-Aldrich	medium
33	BAB	Blood Agar Base	18.78±2.11	0.71±0.12	Sigma-Aldrich	
34	LB	Luria broth	15.11±6	0.67±0.07	Sigma-Aldrich	
35	NB	Nutrient broth	42.67±9.21	0.69±0.03	Sigma-Aldrich	
36	BTSTG	<i>Bacillus thuringiensis</i> spores technical grade	7.13±5.95	0.72±0.12	Agricultural	Bacterial spore with admixtures
37	SB	<i>Saccharomyces boulardii</i>	57.82±7.56	0.69±0.05	Enterol, Biocodex France (*P)	fungi with admixtures
38	SC	<i>Saccharomyces cerevisiae</i>	21.33±5.55	0.76±0.07	Dr. Oetker Germany (*RS)	
39	LS	<i>Lycoperdon</i> spores	14.52±0.62	0.92±0.02	(*OC)	fungal spores
40	JGSS	Johnsons grass smut spores	6.91±0.34	0.98±0.02	Duke Sci. Corp.	smut spore (fungal spore)
41	BGSS	Bermuda grass smut spores	6.47±0.27	0.97±0.02	Duke Sci. Corp.	
42	ACFTD	AC Fine Test Dust	3.47±2.34	0.87±0.09	Duke Sci. Corp.	other
43	NT	Nivea talc	14.33±4.71	0.77±0.09	Nivea Baby (*RS)	
44	PPD	Printer paper dust	76.37±18.89	0.43±0.11	XEROX Laserprint collected from paper shredder (*RS)	
45	PTD	Paper towel dust	73.45±25.65	0.56±0.15	Merida Poland collected from crushed towel (*RS)	
46	CIN	Cinnamon	23.97±4.39	0.78±0.05	Kamis Poland (*RS)	
47	CEL	Celulose	82.86±14.28	0.25±0.04	Sigma-Aldrich	

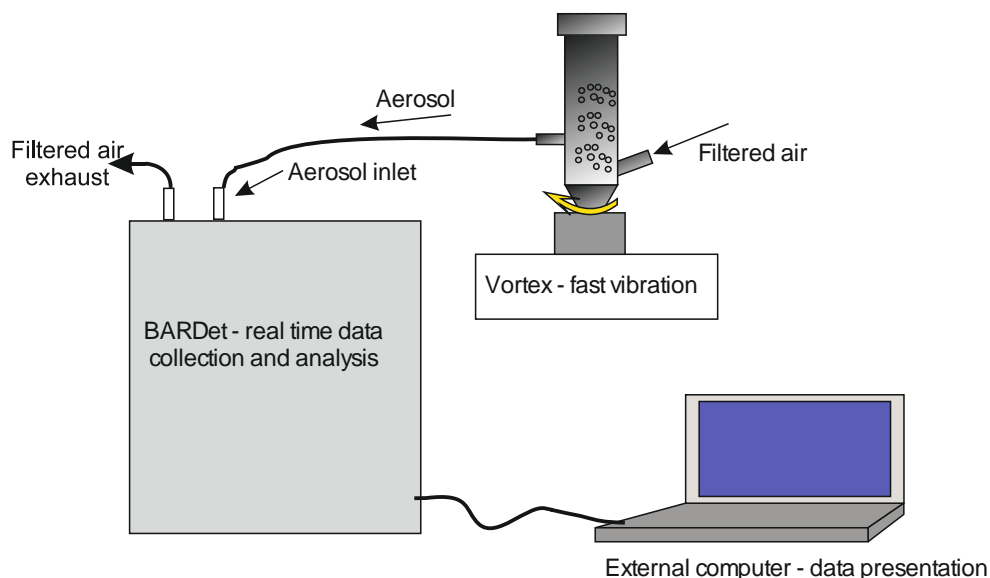
48	GGL	Ground Green Leaves	18.03±4.3	0.77±0.09	Dried and ground Oak (*OC)	
----	-----	---------------------	-----------	-----------	----------------------------	--

134  
135  
136  
137  
138  
139

\*OC – pollens collected from trees, flowers and grass at the region of Warsaw during vegetative seasons in 2015 and 2016.

\*RS – Regular shops in Warsaw where common goods are purchased.

\*P – Pharmacy shops in Warsaw



140  
141  
142

Figure 1. Setup of aerosol generation, data recording and analysis.

### 3.1.3. Aerosol microscopy

144  
145  
146  
147  
148  
149

For microscopy analysis the aerosols were generated as described above and collected by impaction on a glass microscopic slide. The visualization of the samples was performed using a Nikon Eclipse Ti-U microscope with 10x objective. The images were recorded with a 5-megapixel DS-Fi1 camera. The aerosol equivalent diameters and circularity were analyzed automatically using NIS-Elements 64bit 3.22.10 software. The threshold of particle outline was corrected manually to obtain the visually best fit.

150

### 3.1.4. Data acquisition method and pre-processing

152  
153  
154  
155  
156  
157  
158  
159  
160

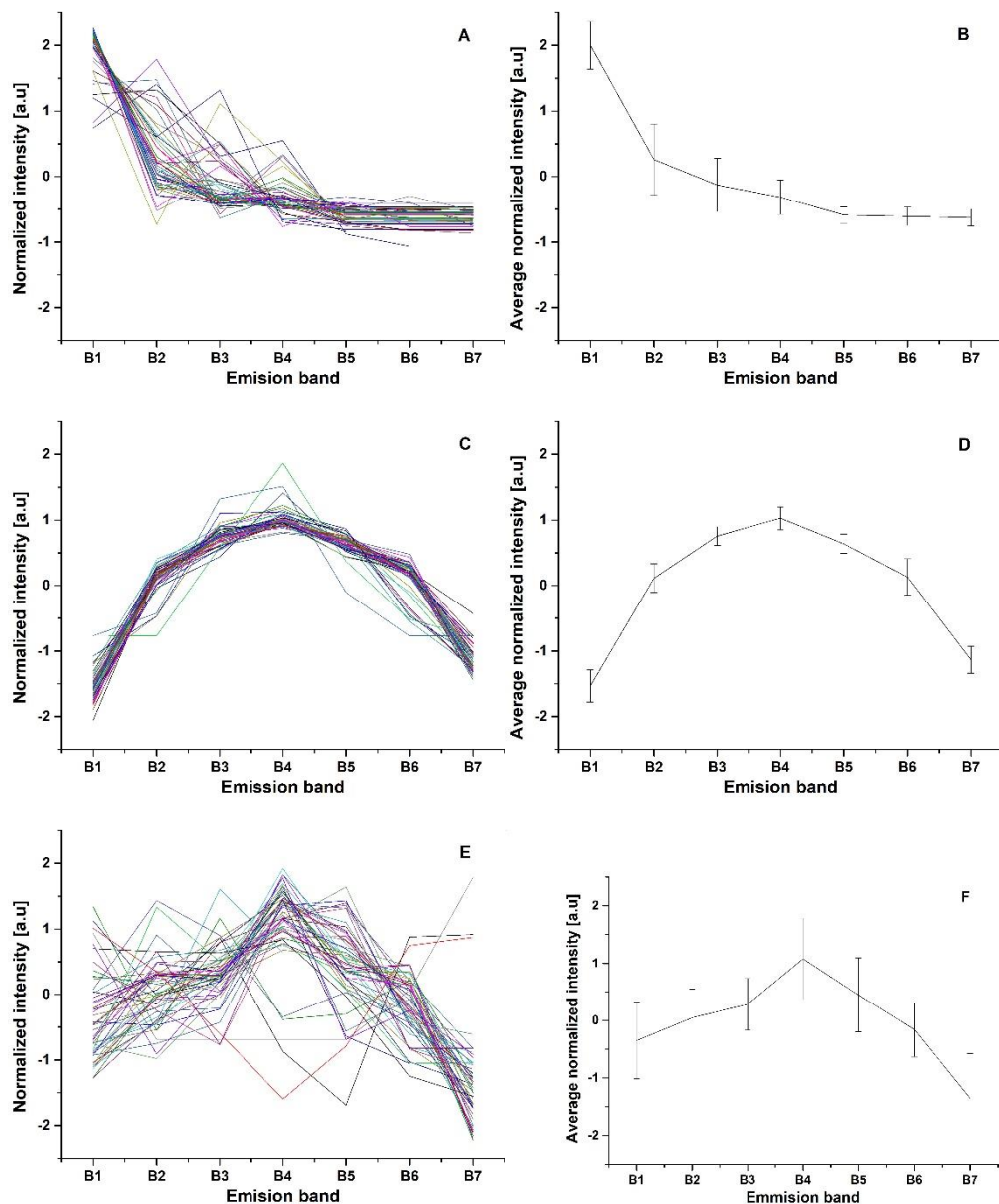
The fluorescence of each particle was recorded in 7 bands. This creates a time series of the signals which has to be pre-processed before further analysis. There are two steps in gathering data. The first one is performed by the internal BARDet's software which is responsible for controlling the instrument and the acquisition of raw signals. Then data is forwarded to a pre-processing module in the analysis software. Its first task is to extract valuable signals from the noise (three sigma rule). After that a normalization procedure is required. It is performed first by subtracting the average value of the signal and then normalizing it to its standard deviation. The main goal was to analyze the shape of the emission spectrum (not signal strength). An example visualization of input data is shown in Figure 2.

161  
162

The data acquisition process started after the stabilization of the aerosol generation rate which was measured by the device. It was important not to exceed one particle per 2 ms of data integration

163 time in a 20 us measurement window. Finally, a total of 114,779 spectral characteristics of 48  
164 aerosols was gathered, which gives on average 2391 (standard deviation 437) fluorescence  
165 characteristics per substance. From the recorded data 80% was used as a training data set and 20% as  
166 a test data set.

167



168

169

170

171 Figure 2. Example, normalized 50 subsequent fluorescence characteristics of NT (A), FM (C) and  
172 LCB (E) and corresponding averaged normalized intensities of NT (B), FM (D) and LCB (F). Error bars  
173 represent standard deviation of measurements.

174

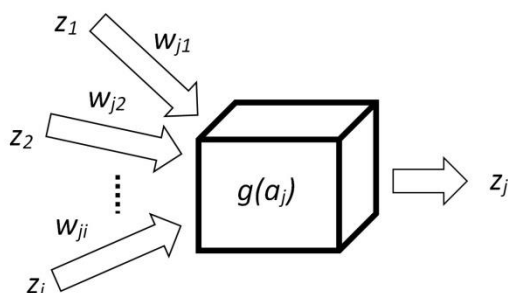
### 175 3.2. Data analysis

#### 176 3.2.1. ANN (Artificial Neural Network)

##### 177 3.2.1.1. Basics

178

179 There are many types of Artificial Neural Networks (ANNs), but in this paper only the  
 180 backpropagation algorithm is demonstrated because it is one of the most practical ones. The main  
 181 concept of this algorithm is based on a model of the neuron that has two tasks. It aggregates signals  
 182 (1) and then processes them by an activation function (2), which, in this research, is a sigmoid. The  
 183 result of such single processing is a new signal  $z_j$  propagated to other neurons (Figure 3).



184  
 185 Figure 3. Mathematical model of single neuron cell.  
 186

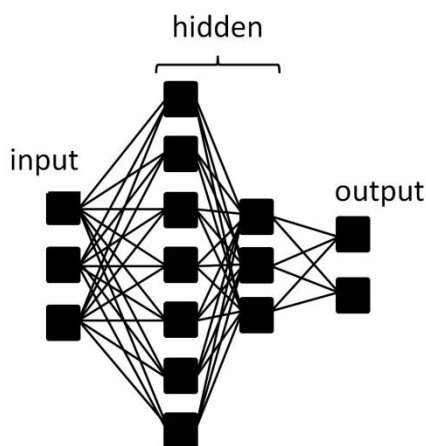
$$a_j = \sum_i w_{ji} z_i \quad (1)$$

187  
 188  $a_j$ - aggregated signal,  $w_{ji}$ - weight that connects neuron  $i$  with  $j$ ,  $z_i$ - signal (input).

$$g(a_j) = \frac{1}{1 + e^{-\beta a_j}} \quad (2)$$

190  
 191  $g(a_j)$  – sigmoidal function,  $\beta$ - parameter (steepness) of sigmoid curve.

192  
 193 The structure of a neural network is formed by layers of neurons: input, hidden and output. In  
 194 this research input neurons constitute a fluorescence spectrum and output neurons represent  
 195 substances. Most computations are carried out in the hidden layers (no more than two layers were  
 196 examined). The schematic representation of neuron layers is presented in Figure 4.



197  
 198 Figure 4. Typical topology of an artificial neural network.  
 199

200 The described algorithm constitutes the supervised learning method that requires training data

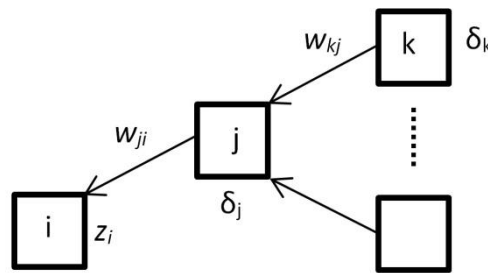


201 for a teaching process. This allows one to calculate an error between the target shown and the ANN  
 202 response. Every problem is related to minimizing output error which is calculated as Mean Squared  
 203 Error (3).

$$E = \frac{1}{2} \sum_{k=1}^c (y_k - t_k)^2 \quad (3)$$

204  $E$  – Mean Squared Error,  $t_k$ - observed value (target),  $y_k$ - calculated response,  $k$ -output neuron,  $c$  –  
 205 number of output neurons.

206 The gradient descent method is used to find a minimum of error function. Error is dependent on  
 207 network weights  $\Delta w_{ji}$  which might be adjusted (4). In order to update weights correctly, firstly one  
 208 needs to propagate error backwards by calculating partial derivatives  $\delta_j$  (5) (Figure 5). All  
 209 mathematical details are well described by C. M. Bishop (Bishop, 1995).



210

211 Figure 5. Model of backward error propagation.

$$\Delta w_{ji}(t) = -\eta \delta_j z_i + m \Delta w_{ji}(t - 1) \quad (4)$$

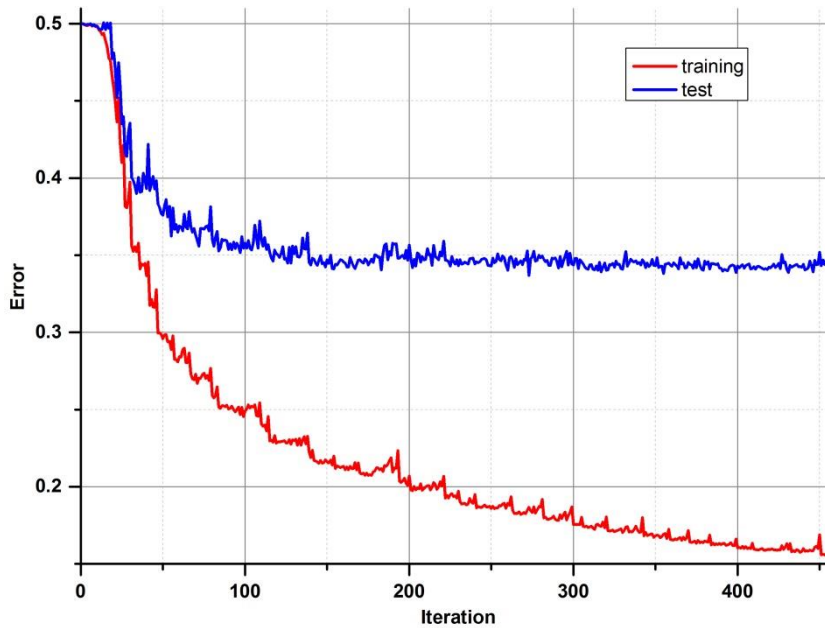
212  $\eta$ - learning rate,  $m$  - momentum,  $t$  - iteration.

213

$$\frac{\delta E}{\delta w_{ji}} = \frac{\delta E}{\delta a_j} \frac{\delta a_j}{\delta w_{ji}} = \delta_j z_i \quad \delta_j = g'(a_j) \sum_k w_{kj} \delta_k \quad (5)$$

214 The learning rate factor determines the size of the steps while the momentum parameter  
 215 enables the local minimum to be omitted by adding a fraction of the weight correction from the last  
 216 step.

217 After the correction of all weights of the ANN, the output error is examined, and the procedure  
 218 starts again unless an error level is low enough and there is no overfitting. All data are divided into  
 219 three different sets: training, test and validation. For calculations during the learning process, only  
 220 the first two are used. In order to determine whether it is time to stop the teaching process, one has  
 221 to observe an error in the test set. There will be a moment when this error comes to be constant or  
 222 starts increasing due to the overfitting of training data (Figure 6). The validation data set may be  
 223 useful for comparing different models or just to verify the current model on a completely separate  
 224 set of data.



225

226 Figure 6. Example of error minimizing during the training process.

227 **3.2.1.2. Implementation of ANN for BARDet**

228 There are statistical commercial software packages available that provide ANN modules as one  
 229 of the methods to analyze the data. It is worthwhile noting that customized software was developed  
 230 for this research. This approach helped us to understand ANNs in depth and led to the development  
 231 of software that is not only responsible for data pre-processing and network training, but also  
 232 (mainly) for solving a real time classification problem.

233 Ruske et al. in their studies (Ruske et al., 2017) compared various algorithms to analyze single  
 234 particle data and noted that an ANN requires much more user input. However, we present a method  
 235 to overcome this inconvenience by automating the process and implementing procedures which  
 236 simplify and improve the analysis.

237 The main disadvantage of an ANN is the fact that it is a parametrized algorithm. How well it  
 238 works depends strictly on a proper choice of the best possible factors, which may be different for  
 239 each problem. There are two types of factors that influence the ANN outcome. The first one  
 240 corresponds to the architecture of the ANN which comprises a number of layers, neurons and an  
 241 activation function parameter. The second one determines the learning process: momentum and  
 242 learning rate. The latter can be tuned during the learning process to make it much faster. The “bold  
 243 driver” procedure was chosen for that purpose. It continuously increases the learning rate unless an  
 244 error is higher from that before the change. If it is, the algorithm radically decreases the learning rate  
 245 and obtains weights from the last step again. Teaching an ANN is a stochastic process initiated by  
 246 using randomly chosen initial weights. It was found that the best procedure for this investigation  
 247 would be to conduct all optimization processes that way. Therefore, the parameters of the ANN,  
 248 responsible both for structure and learning process, are randomly selected until the desired result is  
 249 reached. In fact, the calculations are carried out automatically and simultaneously for several models  
 250 by means of multi core-oriented software. The benefits of this approach are time saving and high  
 251 levels of efficiency and effectiveness in finding the best model. The latter is especially important,  
 252 because the goal is to create a model that produces the best results, which doesn’t necessary mean

253 creating a more complicated network (more neurons or layers).

### 254 **3.2.2. Model evaluation**

255 The main goal of the analysis described in this paper is to find a solution to the bio-aerosol  
256 classification problem. When a training process ends, a final model is created, a network, which has a  
257 unique structure and a set of weights. One can create many of them and make a comparison only by  
258 using the final error. It is not the best solution, because the goal is to distinguish patterns in data  
259 consistently, not to produce a network with a minimal error. That is why there is a need to make a  
260 final analysis of the results and evaluate the model in accordance with the best classification  
261 performance.

262 The standard method for visualization of results is a confusion matrix which will be necessary for  
263 Receiver Operating Characteristics (ROC) analysis (Fawcett, 2006). It simply shows what fraction of  
264 population for each class is predicted correctly or not. Each element from the data set is assigned to  
265 one of the following fits of the confusion matrix: True Positive (TP), True Negative (TN), False  
266 Negative (FN) and False Positive (FP). If it belongs to TP and TN, it was classified correctly.

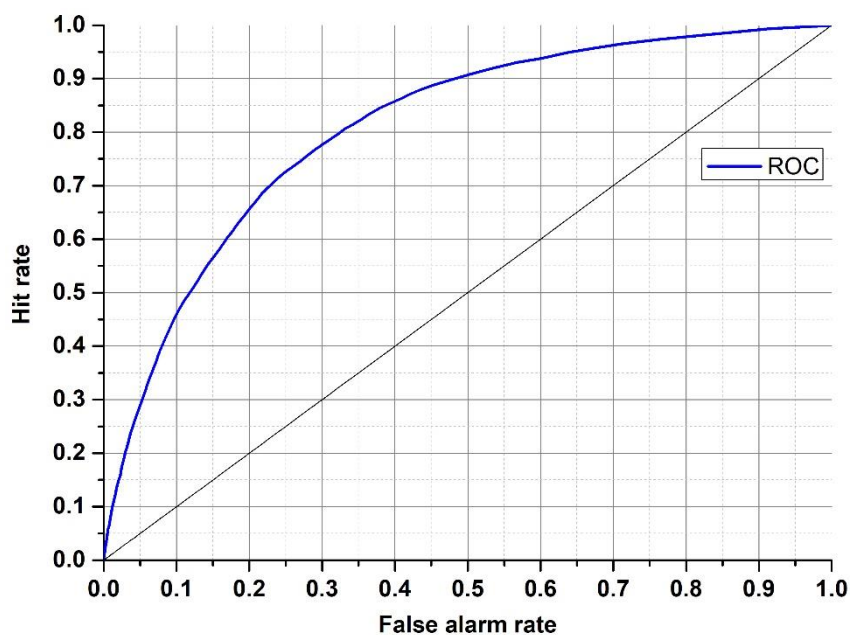
267 The ROC graphs are very simple but useful tools for discovering whether a classifier is worth  
268 using or if it makes a random classification. It is based on two rates from the confusion matrix: hit  
269 rate (6) and false alarm rate (7).

$$\begin{aligned} & \textit{hit rate (true positive rate)} \\ & = \frac{TP}{TP + FN} \end{aligned} \quad (6)$$

270

$$\begin{aligned} & \textit{false alarm rate (false positive rate)} \\ & = \frac{FP}{FP + TN} \end{aligned} \quad (7)$$

271 Each discrete classifier has a threshold level that assigns an element to a positive or negative  
272 class. The points on the ROC graph (Figure 7) represent the classifier for many thresholds. The most  
273 desirable curve will be obtained when the true positive rate is high, and the false positive rate is low  
274 (convex line). The random classifier, in turn, has a hit rate equal to a false alarm rate despite  
275 threshold variation (diagonal line). To identify an ROC analysis with one coefficient, the area under  
276 the curve (AUC) may be used. The higher value of AUC results in better performance (0.5 means  
277 random, 1 - excellent).



278

279 Figure 7. ROC graph with an example of classifier (blue).

280 The confusion matrix and ROC analysis described above were defined for two class problems  
 281 (positive, negative). There is a straightforward way to expand it for multi-class problems. One needs  
 282 to take a desired class versus all other classes. Then it will be possible to compare how good the  
 283 classifier for specific classes within one model is.

#### 284 4. Results

##### 285 4.2. ANN performance

286 The first attempts were made to distinguish all substances using only one neural network model.  
 287 The tests revealed that it is impossible due to the huge number of samples (48 aerosols) and only a  
 288 few of them presented significantly different fluorescence spectra which allow accurate  
 289 characterization. The remaining substances are then misclassified. Therefore, we decided to use a  
 290 more practical approach to this problem, which would be to create several groups (considering  
 291 information about aerosols), but we did not want to make any classes *a priori*. Although the ANN  
 292 type demonstrated needs training, which requires a set of known classes, further tests showed that  
 293 there is a possibility of finding similarities between substances through the analysis of confusion  
 294 matrices. It was achieved after many trials of matching substances, which were not well separated,  
 295 into new groups and checking if they are good enough on ROC graphs. Consequently, this procedure  
 296 was also applied to those new groups.

297

298 All examples demonstrated below were calculated on the test data sets, not training data. In the  
 299 first presented (Figure 8), which tries to classify all of the 48 substances (group 0), four aerosols  
 300 reached a very high accuracy of separation (AUC>0,9). The best separation was achieved for  
 301 fluorescent microspheres (FM). In this case 98.5% of all FM particles were correctly classified.  
 302 Similarly, an efficient separation was achieved for riboflavin (RIB), Talc (NT) and *Lactobacillus*  
 303 *bulgaricus* (LCB). The remaining aerosols were divided into 3 separate groups that gather the most  
 304 similar substances (group 1-3) (Table 3). The subsequent groups up to 21 represent individual ANNs  
 305 leading to the final classification of the aerosol. In practice separation is done not by one confusion  
 306 matrix (ANN) but by all of them in sequence (22 ANNs combined in a decision tree). For example, if

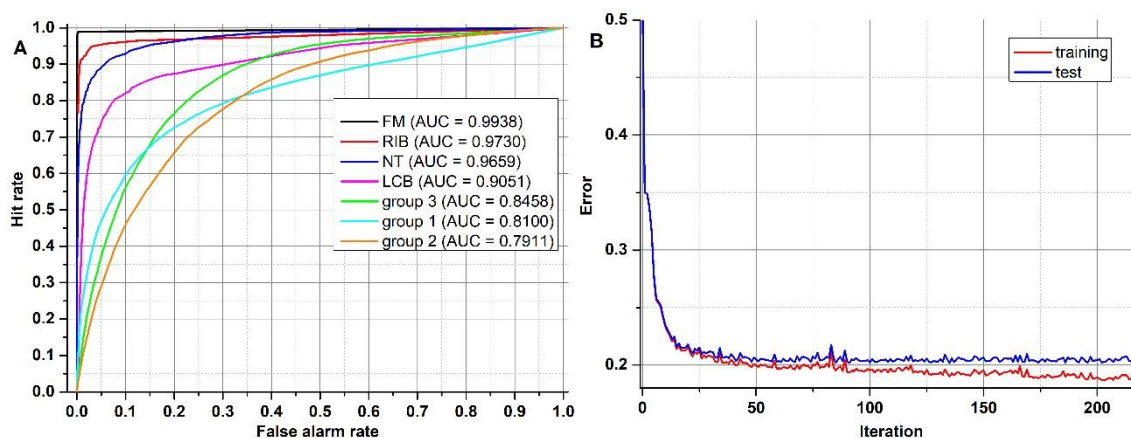
307 an ANN classifies unknown substance into any of 22 groups it means that decision process is not  
 308 ended but from that moment another ANN classifies this substance. However, each new ANN is  
 309 trained using only a subsection of the data excluding the data from other groups.

310

311 Table 3. Exemplary confusion matrix of all aerosols classified by the first ANN.

312

		predicted						
		FM	RIB	NT	LCB	group 3	group 1	group 2
true	FM	98.5	0	0	0.3	0.1	0	1.1
	RIB	0.1	91	0.5	3.1	1.2	0.6	3.4
	NT	0	0.1	86.5	0	9.3	0.3	3.8
	LCB	1	1.6	0.6	72.7	3.9	10.7	9.5
	group 3	0	0.7	6.6	0.6	63.3	12	16.8
	group 1	0.2	1	1	7.9	12.5	61.6	15.8
	group 2	0.1	1.2	3.8	6.6	17.6	13.2	57.4



313

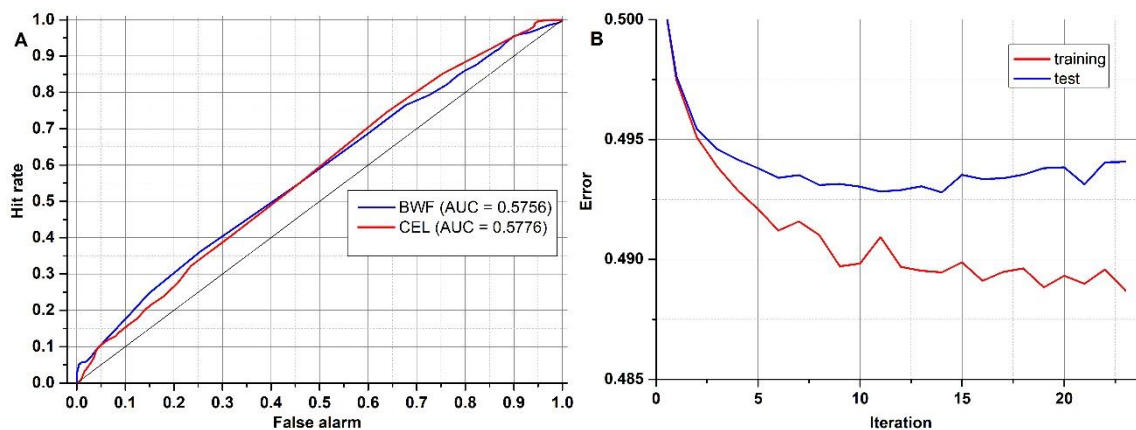
314 Figure 8. (A) ROC and (B) error progress of ANN that classifies all samples.

315 Table 4 and Figure 9 show results achieved for two substances that have a very similar spectrum  
 316 and the AUCs calculated are not much higher than in a random classifier. This example clearly shows  
 317 why we are not always able to classify every single particle of aerosol with 100% accuracy. However,  
 318 just a representative number (several dozen) of measured particles (a cloud) allows the proper  
 319 prediction of aerosol types within a few seconds. This is easy to observe during real time detection,  
 320 because counts allocated in a confusion matrix tend to reach a stable state quite quickly.

321

		predicted	
		BWF	CEL
true	BWF	54.8	45.2
	CEL	45.6	54.4

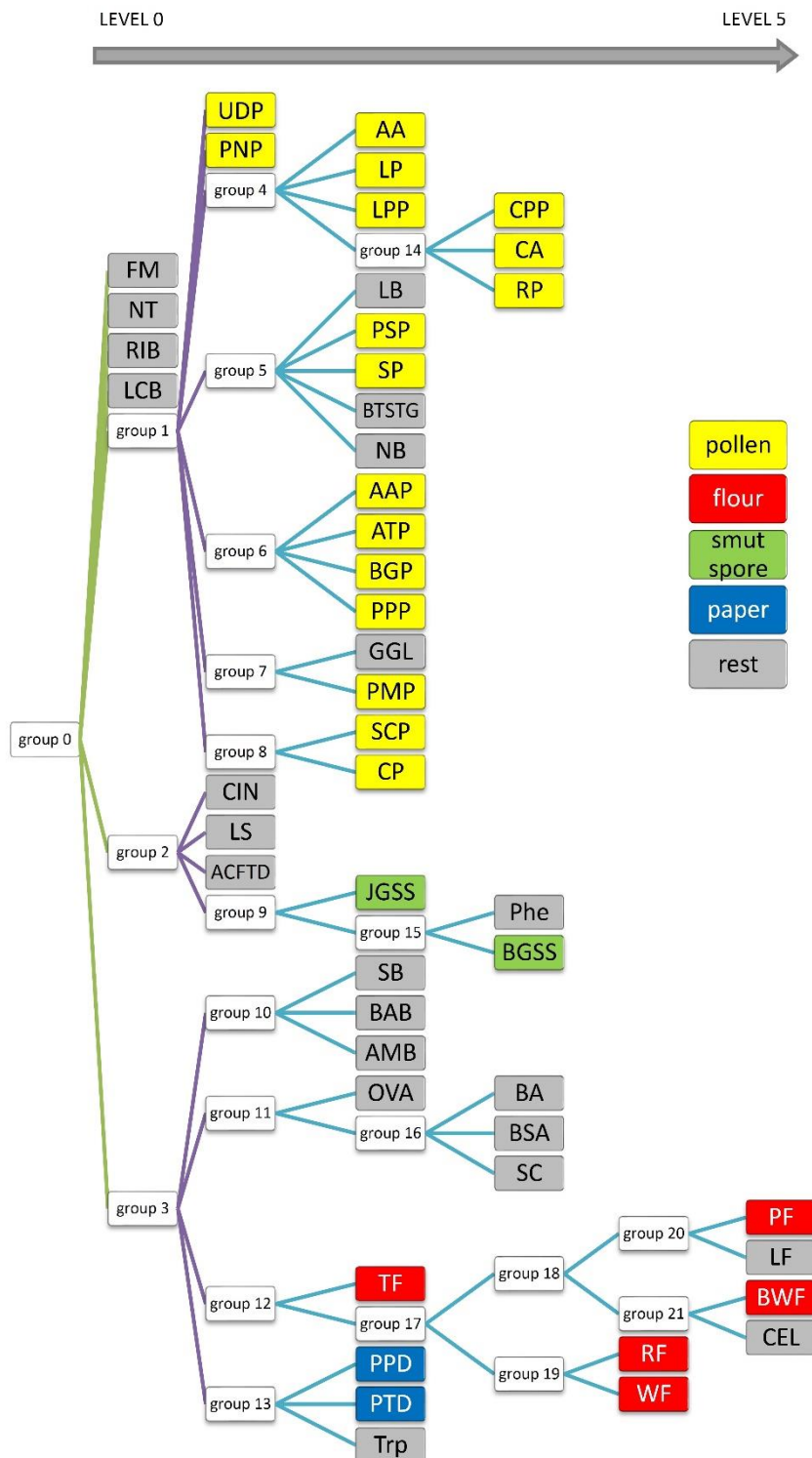
322 Table 4. Confusion matrix of two substances that have very similar spectra.



323  
 324 Figure 9. ROC (A) and error progress (B) of ANN which classify two very similar samples.

325  
 326 **4.3. Classification tree**

327 Finally, to achieve the best possible classification, a decision tree was created (Figure 10). It  
 328 comprises not one, but 22 models. The process of creating them is not replicable in terms of the  
 329 exact factors used for ANN generation. However, this is not essential, because the decision tree is  
 330 based on ANN results (classification ability), which should be possibly the highest. Therefore, the final  
 331 result will be the same. It is difficult to present confusion matrices and ROC graphs for all neural  
 332 networks in this paper. Therefore, only the most interesting one has been discussed. Here, each node  
 333 represents a network that classifies a group of aerosols. The aerosols on the left side of the diagram  
 334 show the most distinct differences, thus they are easy to classify (Level 0). On the right side (Level 1-  
 335 5), this task is much more demanding due to a similar spectrum and the separation is less probable in  
 336 accordance with single particles, although it is still very useful from a practical point of view for  
 337 aerosol cloud discrimination.



338

339 Figure 10. The decision tree consists of 22 ANNs separating 48 substances.

340

341

342

343

344

345

At first glance one can see that FM and RIB are very well recognized, but that was expected because these are standards of fluorescence. Surprisingly, NT and LCB aerosols were also separated from the others (level 0 network). Further analysis of the tree structure identifies a correlation between samples and their real categories. It is especially noticeable for pollens, which are allocated to a separate branch of that tree, and all stems from group 1. Most of them were classified on the third level. Interestingly all grass pollens (AAP, ATP, BGP, PPP) belong to the same group, 6. Similarly,

346 both *Lycopodium* pollens from different regions of the world show a close correlation, although *Abies*  
347 *alba*, which is a tree, was classified in the same group. Flours, Smut Spores and Papers are dispersed  
348 between different levels, but particular groups belong to the same branch of the tree. However, some  
349 of the samples are scattered on the whole tree area and do not correspond to any group.

350 It should be noted that the result is a system of 22 ANNs that work simultaneously. In  
351 comparison to the training process, which is rather time consuming and has to be empirically  
352 optimized, this cluster of learned ANNs delivers high performance. Input data is processed by a single  
353 ANN in milliseconds. This performance makes the neural network a great tool as a splitting node in  
354 the classification tree. Compared to our previous results, where Principal Component Analysis was  
355 applied to analyze data from BARDet (Kaliszewski et al., 2016), the ANNs allowed much better  
356 discrimination between various bio-aerosols.

## 357 5. Summary

358 In this paper the possibility of applying an Artificial Neural Network (ANN) for real time  
359 classification of biological aerosols was investigated. The spectral characteristics of bio-aerosols were  
360 collected using the BARDet instrument. The database consisted of 48 substances. Finally, 22 neural  
361 networks were trained and combined into a decision tree. This allowed aerosols to be  
362 characterized in real time. Tests revealed that only certain substances have such characteristic  
363 fluorescence spectra that allow correct classification of almost each particle. However, in all other  
364 cases the system was able to recognize a particular aerosol accurately with no mistake, but a  
365 representative number of several dozens of particles in a cloud was necessary. Further  
366 approximation was based on decision tree analysis where each node corresponded to a separate  
367 learned ANN. The best sets of ANNs for each group of similar aerosols were discovered utilizing  
368 confusion matrices and ROC analysis. Our intention was to make a complete system which detects  
369 and classifies substances without creating groups *a priori*. This attitude helped us to create a  
370 powerful analytical tool that works automatically, and the results of classification are immediately  
371 available on the operator's screen.

372 This study proved that it is possible to create a tool for a highly effective analysis of bio-aerosols  
373 using multiple ANNs combined into a decision tree. Our approach allowed us to automate and speed  
374 up the analysis, which reduced time and the amount of computing power needed. In a future study  
375 the database will be extended to obtain potentially a vast variety of samples including  
376 atmospherically relevant bacteria and fungi. In the next step, the actual performance of the system  
377 will be determined under real environmental conditions, which will be most challenging due to the  
378 presence of unknown fluorescent and non-fluorescent particles.

379

## 380 Data availability

381 The experimental aerosol data can be provided upon request. The software for automatic data  
382 analysis cannot be publicly provided at this moment since it is a subject of negotiations with a  
383 company.

384

## 385 Acknowledgments

386 The work presented was supported by a grant from The National Centre of Research and  
387 Development (Poland), within the project "Mobile laboratory for environmental sampling and  
388 identification of biological threats" (O ROB 0031 01/ID/31/1).

389



390 **References**

- 391 Agranovski, V., Ristovski, Z., Hargreaves, M., Blackall, P. J. and Morawska, L.: Performance  
392 evaluation of the UVAPS: Influence of physiological age of airborne bacteria and bacterial  
393 stress, *J. Aerosol Sci.*, 34(12), 1711–1727, doi:10.1016/S0021-8502(03)00191-5, 2003.
- 394 Antowiak, M. and Asińska-macukow, K. C. H. a: Fingerprint identification by using artificial  
395 neural network with optical wavelet preprocessing, , 11(4), 327–337, 2003.
- 396 Purnomo, H. D., Hartomo, K. D. and Prasetyo, S. Y. J.: Artificial Neural Network for Monthly  
397 Rainfall Rate Prediction , *IOP Conf. Ser. Mater. Sci. Eng.*, 180(1), 12057, doi:10.1088/1742-  
398 6596/755/1/011001, 2017.
- 399 Bhangar, S., Huffman, J. A. and Nazaroff, W. W.: Size-resolved fluorescent biological aerosol  
400 particle concentrations and occupant emissions in a university classroom, *Indoor Air*, 24(6),  
401 604–617, doi:10.1111/ina.12111, 2014.
- 402 Bishop, C. M.: Neural networks for pattern recognition, Oxford University Press, Inc., New  
403 York, NY, USA., 1995.
- 404 Blais-Lecours, P., Perrott, P. and Duchaine, C.: Non-culturable bioaerosols in indoor settings:  
405 Impact on health and molecular approaches for detection, *Atmos. Environ.*, 110, 45–53,  
406 doi:10.1016/j.atmosenv.2015.03.039, 2015.
- 407 Borecki, M., Korwin-Pawłowski, M. L. and Beblowska, M.: A method of examination of liquids  
408 by neural network analysis of reflectometric and transmission time domain data from optical  
409 capillaries and fibers, in *IEEE Sensors Journal*, vol. 8, pp. 1208–1214., 2008.
- 410 Choi, K., Ha, Y., Lee, H. K. and Lee, J.: Development of a biological aerosol detector using  
411 laser-induced fluorescence and a particle collection system, *Instrum. Sci. Technol.*, 42(2),  
412 200–214, doi:10.1080/10739149.2013.855639, 2014.
- 413 Crawford, I., Ruske, S., Topping, D. O. and Gallagher, M. W.: Evaluation of hierarchical  
414 agglomerative cluster analysis methods for discrimination of primary biological aerosol,  
415 *Atmos. Meas. Tech.*, 8(11), 4979–4991, doi:10.5194/amt-8-4979-2015, 2015.
- 416 Davidson, C. I., Phalen, R. F. and Solomon, P. A.: Airborne particulate matter and human  
417 health: A review, *Aerosol Sci. Technol.*, 39(8), 737–749, doi:10.1080/02786820500191348,  
418 2005.
- 419 Deguillaume, L., Leriche, M., Amato, P., Ariya, P. a., Delort, A. M., Pöschl, U., Chaumerliac, N.,  
420 Bauer, H., Flossmann, a. I. and Morris, C. E.: Microbiology and atmospheric processes:  
421 chemical interactions of Primary Biological Aerosols, *Biogeosciences Discuss.*, 5(1), 841–870,  
422 doi:10.5194/bgd-5-841-2008, 2008.
- 423 Fawcett, T.: An introduction to ROC analysis. *Pattern Recognition Letters*, *Pattern Recognit.*  
424 *Lett.*, 27(8), 861–874, doi:https://doi.org/10.1016/j.patrec.2005.10.010, 2006.
- 425 Fennelly, M. J., Sewell, G., Prentice, M. B., O'Connor, D. J. and Sodeau, J. R.: Review: The use  
426 of real-time fluorescence instrumentation to monitor ambient primary biological aerosol  
427 particles (PBAP), *Atmosphere (Basel)*., 9(1), doi:10.3390/atmos9010001, 2017.
- 428 Feugnet, G., Lallier, E., Grisard, A., McIntosh, L., Hellström, J. E., Jelger, P., Laurell, F., Albano,  
429 C., Kaliszewski, M., Włodarski, M., Mlynczak, J., Kwasny, M., Zawadzki, Z., Mierczyk, Z.,  
430 Kopczynski, K., Rostedt, A., Putkiranta, M., Marjamäki, M., Keskinen, J., Enroth, J., Janka, K.,

431 Reinivaara, R., Holma, L., Humppi, T., Battistelli, E., Iliakis, E. and Gerolimos, G.: Improved  
432 laser-induced fluorescence method for bio-attack early warning detection system, in  
433 Proceedings of SPIE - The International Society for Optical Engineering, vol. 7116, p. 71160C,  
434 Thales Research and Technology, France., 2008.

435 Fröhlich-Nowoisky, J., Kampf, C. J., Weber, B., Huffman, J. A., Pöhlker, C., Andreae, M. O.,  
436 Lang-Yona, N., Burrows, S. M., Gunthe, S. S., Elbert, W., Su, H., Hoor, P., Thines, E.,  
437 Hoffmann, T., Després, V. R. and Pöschl, U.: Bioaerosols in the Earth system: Climate, health,  
438 and ecosystem interactions, *Atmos. Res.*, 182, 346–376,  
439 doi:10.1016/j.atmosres.2016.07.018, 2016.

440 Fuzzi, S., Baltensperger, U., Carslaw, K., Decesari, S., Denier Van Der Gon, H., Facchini, M. C.,  
441 Fowler, D., Koren, I., Langford, B., Lohmann, U., Nemitz, E., Pandis, S., Riipinen, I., Rudich, Y.,  
442 Schaap, M., Slowik, J. G., Spracklen, D. V., Vignati, E., Wild, M., Williams, M. and Gilardoni, S.:  
443 Particulate matter, air quality and climate: Lessons learned and future needs, *Atmos. Chem.*  
444 *Phys.*, 15(14), 8217–8299, doi:10.5194/acp-15-8217-2015, 2015.

445 Gabey, A. M., Gallagher, M. W., Whitehead, J., Dorsey, J. R., Kaye, P. H. and Stanley, W. R.:  
446 Measurements and comparison of primary biological aerosol above and below a tropical  
447 forest canopy using a dual channel fluorescence spectrometer, *Atmos. Chem. Phys.*, 10(10),  
448 4453–4466, doi:10.5194/acp-10-4453-2010, 2010.

449 Gabey, A. M., Stanley, W. R., Gallagher, M. W. and Kaye, P. H.: The fluorescence properties  
450 of aerosol larger than 0.8  $\mu$  in urban and tropical rainforest locations, *Atmos. Chem. Phys.*,  
451 11(11), 5491–5504, doi:10.5194/acp-11-5491-2011, 2011.

452 Górný, R. L.: Filamentous microorganisms and their fragments in indoor air - A review, *Ann.*  
453 *Agric. Environ. Med.*, 11(2), 185–197, doi:10.1007/BF02677055, 2004.

454 Hernandez, M., Perring, A. E., McCabe, K., Kok, G., Granger, G. and Baumgardner, D.:  
455 Chamber catalogues of optical and fluorescent signatures distinguish bioaerosol classes,  
456 *Atmos. Meas. Tech.*, 9(7), 3283–3292, doi:10.5194/amt-9-3283-2016, 2016.

457 Hill, S. C., Pinnick, R. G., Niles, S., Pan, Y.-L., Holler, S., Chang, R. K., Bottinger, J., Chen, B. T.,  
458 Orr, C.-S. and Feather, G.: Realtime Measurement of Fluorescence Spectra from Single  
459 Airborne Biological Particles, *F. Anal. Chem. Technol.*, 3(4–5), 221–239,  
460 doi:10.1002/(SICI)1520-6521(1999)3:4/5<221::AID-FACT2>3.3.CO;2-Z, 1999.

461 Huffman, J. A., Treutlein, B. and Pöschl, U.: Fluorescent biological aerosol particle  
462 concentrations and size distributions measured with an Ultraviolet Aerodynamic Particle  
463 Sizer (UV-APS) in Central Europe, *Atmos. Chem. Phys.*, 10(7), 3215–3233, doi:10.5194/acp-  
464 10-3215-2010, 2010.

465 Kaliszewski, M., Trafny, E. A., Lewandowski, R., Włodarski, M., Bombalska, A., Kopczyński, K.,  
466 Antos-Bielska, M., Szpakowska, M., Młyńczak, J., Mularczyk-Oliwa, M. and Kwaśny, M.: A  
467 new approach to UVAPS data analysis towards detection of biological aerosol, *J. Aerosol Sci.*,  
468 58, 148–157, doi:10.1016/j.jaerosci.2013.01.007, 2013.

469 Kaliszewski, M., Włodarski, M., Młyńczak, J., Leśkiewicz, M., Bombalska, A., Mularczyk-Oliwa,  
470 M., Kwaśny, M., Buliński, D. and Kopczyński, K.: A new real-time bio-aerosol fluorescence  
471 detector based on semiconductor CW excitation UV laser, *J. Aerosol Sci.*, 100, 14–25,  
472 doi:10.1016/j.jaerosci.2016.05.004, 2016.

473 Kohlus, R. and Bottlinger, M.: Particle Shape Analysis as an example of knowledge extraction

474 by neural nets, Part. Part. Syst. Charact., 10(5), 275–278, doi:10.1002/ppsc.19930100511,  
475 1993.

476 Lakowicz, J. R.: Principles of fluorescence spectroscopy, Second., Kluwer Academic/Plenum  
477 Publishers., 2006.

478 Leśkiewicz, M., Kaliszewski, M., Mierczyk, Z. and Włodarski, M.: Comparison of Principal  
479 Component Analysis and Linear Discriminant Analysis applied to classification of excitation-  
480 emission matrices of the selected biological material, Biul. Wojsk. Akad. Tech., 65(1), 15–31,  
481 doi:10.5604/12345865.1197960, 2016.

482 Lim, D. V., Simpson, J. M., Kearns, E. A. and Kramer, M. F.: Current and developing  
483 technologies for monitoring agents of bioterrorism and biowarfare, Clin. Microbiol. Rev.,  
484 18(4), 583–607, doi:10.1128/CMR.18.4.583-607.2005, 2005.

485 Mauderly, J. L. and Chow, J. C.: Health effects of organic aerosols, Inhal. Toxicol., 20(3), 257–  
486 288, doi:10.1080/08958370701866008, 2008.

487 Miaskiewicz-Peska, E. and Lebkowska, M.: Comparison of aerosol and bioaerosol collection  
488 on air filters, Aerobiologia (Bologna), 28(2), 185–193, doi:10.1007/s10453-011-9223-1,  
489 2012.

490 Michaels, R. A.: Environmental Moisture, Molds, and Asthma—Emerging Fungal Risks in the  
491 Context of Climate Change, Environ. Claims J., 29(3), 171–193,  
492 doi:10.1080/10406026.2017.1345521, 2017.

493 Pan, Y. Le, Hill, S. C., Pinnick, R. G., House, J. M., Flagan, R. C. and Chang, R. K.: Dual-  
494 excitation-wavelength fluorescence spectra and elastic scattering for differentiation of single  
495 airborne pollen and fungal particles, Atmos. Environ., 45(8), 1555–1563,  
496 doi:10.1016/j.atmosenv.2010.12.042, 2011.

497 Pan, Y. Le, Huang, H. and Chang, R. K.: Clustered and integrated fluorescence spectra from  
498 single atmospheric aerosol particles excited by a 263- and 351-nm laser at New Haven, CT,  
499 and Adelphi, MD, J. Quant. Spectrosc. Radiat. Transf., 113(17), 2213–2221,  
500 doi:10.1016/j.jqsrt.2012.07.028, 2012.

501 Pinnick, R. G., Hill, S. C., Pan, Y. Le and Chang, R. K.: Fluorescence spectra of atmospheric  
502 aerosol at Adelphi, Maryland, USA: Measurement and classification of single particles  
503 containing organic carbon, Atmos. Environ., 38(11), 1657–1672,  
504 doi:10.1016/j.atmosenv.2003.11.017, 2004.

505 Pöhlker, C., Huffman, J. A. and Pöschl, U.: Autofluorescence of atmospheric bioaerosols:  
506 Spectral fingerprints and taxonomic trends of pollen, Atmos. Meas. Tech., 6(12), 3369–3392,  
507 doi:10.5194/amt-6-3369-2013, 2013.

508 Pope, C. A. and Dockery, D. W.: Health effects of fine particulate air pollution: Lines that  
509 connect, J. Air Waste Manag. Assoc., 56(6), 709–742, doi:10.1080/10473289.2006.10464485,  
510 2006.

511 Pósfai, M. and Buseck, P. R.: Nature and Climate Effects of Individual Tropospheric Aerosol  
512 Particles, Annu. Rev. Earth Planet. Sci., 38(1), 17–43,  
513 doi:10.1146/annurev.earth.031208.100032, 2010.

514 Ruske, S., Topping, D. O., Foot, V. E., Kaye, P. H., Stanley, W. R., Crawford, I., Morse, A. P. and  
515 Gallagher, M. W.: Evaluation of machine learning algorithms for classification of primary

516 biological aerosol using a new UV-LIF spectrometer, *Atmos. Meas. Tech.*, 10(2), 695–708,  
517 doi:10.5194/amt-10-695-2017, 2017.

518 Savage, N. J., Krentz, C. E., Könemann, T., Han, T. T., Mainelis, G., Pöhlker, C. and Alex  
519 Huffman, J.: Systematic characterization and fluorescence threshold strategies for the  
520 wideband integrated bioaerosol sensor (WIBS) using size-resolved biological and interfering  
521 particles, *Atmos. Meas. Tech.*, 10(11), 4279–4302, doi:10.5194/amt-10-4279-2017, 2017.

522 Shiraiwa, M., Selzle, K. and Pöschl, U.: Hazardous components and health effects of  
523 atmospheric aerosol particles: Reactive oxygen species, soot, polycyclic aromatic compounds  
524 and allergenic proteins, *Free Radic. Res.*, 46(8), 927–939,  
525 doi:10.3109/10715762.2012.663084, 2012.

526 Taketani, F., Kanaya, Y., Nakamura, T., Koizumi, K., Moteki, N. and Takegawa, N.:  
527 Measurement of fluorescence spectra from atmospheric single submicron particle using  
528 laser-induced fluorescence technique, *J. Aerosol Sci.*, 58, 1–8,  
529 doi:10.1016/j.jaerosci.2012.12.002, 2013.

530 Trafny, E. A., Lewandowski, R., Stępińska, M. and Kaliszewski, M.: Biological threat detection  
531 in the air and on the surface: How to define the risk, *Arch. Immunol. Ther. Exp. (Warsz.)*,  
532 62(4), 253–261, doi:10.1007/s00005-014-0296-8, 2014.

533 Uk Lee, B., Jung, J. H., Yun, S. H., Hwang, G. B. and Bae, G. N.: Application of UVAPS to real-  
534 time detection of inactivation of fungal bioaerosols due to thermal energy, *J. Aerosol Sci.*,  
535 41(7), 694–701, doi:10.1016/j.jaerosci.2010.04.003, 2010.